The Egyptian Journal of Radiology and Nuclear Medicine (2014) **45**, 75–87

Egyptian Society of Radiology and Nuclear Medicine

The Egyptian Journal of Radiology and Nuclear Medicine

www.elsevier.com/locate/ejrnm
www.sciencedirect.com

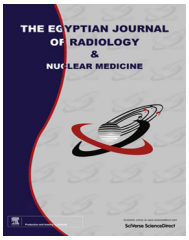

ORIGINAL ARTICLE

Can real-time ultrasound elastography using the color score and strain ratio differentiate between benign and malignant solitary thyroid nodules?

Rania Refaat [a,*], **Amr Kamel** [b], **Mahmoud Elganzory** [b], **Nahla M. Awad** [c]

[a] *Department of Radiodiagnosis, Ain Shams University, Cairo, Egypt*
[b] *Department of Surgery, Ain Shams University, Cairo, Egypt*
[c] *Early Cancer Detection Unit of Cytology and Pathology, Ain Shams University Hospitals, Cairo, Egypt*

Received 15 September 2013; accepted 8 December 2013
Available online 22 January 2014

KEYWORDS

Real-time ultrasound elastography (USE);
Benign solitary thyroid nodules;
Malignant solitary thyroid nodules;
Rago criteria;
Histopathological examination

Abstract *Background:* Solitary thyroid nodule may represent a multitude of thyroid disorders; therefore, detection of whether these nodules are benign or malignant is crucial for patient's triage.
Objective: To evaluate the diagnostic performance of the latest generation of real-time ultrasound elastography (USE) in differentiation between benign and malignant solitary thyroid nodules.
Materials and methods: Thirty consecutive patients who were referred for surgical treatment were prospectively examined by real-time USE. Tissue stiffness on real-time USE was determined with light compression using the standard elastography color scoring system according to Rago criteria ranging from 1 (low stiffness over the entire nodule) to 5 (high stiffness over the entire nodule and surrounding tissue). The strain ratio (normal tissue to lesion strain ratio) was calculated. The histopathological examination of these resected nodules was used as the diagnostic standard of reference.
Results: Scores of 1 and 2 with Rago criteria were highly significant seen in benign nodules, whereas, scores of 4 and 5 with Rago criteria were highly significant seen in malignant nodules ($p < 0.001$) with a sensitivity, specificity and diagnostic accuracy of 78.6%, 78.9% and 78.8% respectively. Additionally, the best strain ratio cut-off value for discrimination between benign and malignant nodules by using receiver operating characteristic analysis was 2.20 (area under the curve of 0.861; p value < 0.001) with a consequential sensitivity, specificity and diagnostic accuracy of 85.7%, 90.5% and 88.6% respectively.
Conclusion: Both the color score and the strain ratio are higher in malignant solitary thyroid nodules than those in benign ones. Consequently, real-time USE can be used for the differentiation of benign and malignant solitary thyroid nodules. Eventually, this reduces the number of superfluous surgical procedures on benign thyroid nodules.

* Corresponding author. Mobile: +2 01005285089.
E-mail address: raniarefaat_1977@hotmail.com (R. Refaat).
Peer review under responsibility of Egyptian Society of Radiology and Nuclear Medicine.

ELSEVIER Production and hosting by Elsevier

1. Introduction

Thyroid nodules are a common finding in the general population (1). The number of thyroid nodules is increasing as they are incidentally detected during imaging studies indicated for non thyroid reasons. Additionally, most incidentally detected

0378-603X © 2014 Production and hosting by Elsevier B.V. on behalf of Egyptian Society of Radiology and Nuclear Medicine.
Open access under CC BY-NC-ND license. http://dx.doi.org/10.1016/j.ejrnm.2013.12.005

thyroid nodules are asymptomatic and benign; however, it is clinically important to diagnose malignant nodules (2) which account to 5% of thyroid nodules (3). Understanding the etiology of nodular thyroid disease is a fundamental prerequisite for its subsequent eradication (4).

Guidelines generally recommend the use of functional and morphological characterization using a combination of clinical examination, diagnostic imaging and fine-needle aspiration biopsy (FNAB) for the latter (5). FNAB is the best method to differentiate between benign and malignant thyroid nodules, yet, it suffers the limitations of being invasive and sampling errors are inevitable (6). FNAB is also a time-intensive procedure as it requires sending to and evaluation of the sample by the pathologist (7). On the other hand, ultrasound (US) is a non invasive and easily available imaging technique for the evaluation of thyroid nodules (8).

It is generally believed that US criteria such as hypoechogenicity, the lack of a complete halo surrounding the nodule (irregular margins), microcalcifications, more tall than wide shape and marked intranodular and absent or slight perinodular vascularization using Doppler-flow (type III flow) are helpful in targeting nodules at the highest risk of harboring thyroid malignancy (3,5). Moreover, each characteristic increases the sensitivity in a number of combinations; nevertheless, this lacks adequate specificity for reliably diagnosing thyroid malignancy (9).

Conversely, palpation is a basic and important method in the assessment of thyroid nodules (10) as a firm and hard thyroid nodule on palpation is associated with an increased risk of malignancy (5). Nevertheless, palpation is subjective and highly dependent on the examiner (11). Gray-scale US does not provide direct information corresponding to the hardness of a nodule (10). During the last few years, a novel promising imaging technology based on the elastic property of the tissue, USE has been added to the diagnostic armamentarium (9). This is done by measuring the tissue strain induced non invasively by compression (10,12).

Accordingly, the objective of our study was to evaluate the diagnostic performance of the latest generation of real-time USE as an individual variable in differentiation between benign and malignant solitary thyroid nodules using the histopathological diagnosis of the resected thyroid nodules as the reference standard. Therefore, other ultrasound criteria, such as the echogenicity and perfusion pattern of individual nodules, are purposely not taken into account.

2. Patients

This is a prospective study conducted from December 2012 to July 2013 in which 30 consecutive patients with solitary thyroid nodules who were referred for surgical treatment were included. Patients with multiple thyroid nodules (more than two nodules), previous surgery or radioiodine therapy and patients with thyroid nodules who refused or had any contraindication for thyroid surgery were excluded from our study. Patients with purely cystic (anechoic nodules without solid components) and egg shell-calcified nodules were also on our exclusion list because of posterior enhancement or posterior shadow artifacts of ultrasound imaging that could cause color-coding problems. Additionally, patients with nodules of greatest diameter larger than 40 mm were excluded because insufficient normal thyroid tissue around the targeted nodule ensues difficulties in measuring thyroid nodule elasticity whether by the elastography color scoring system or by calculation of the strain ratio. As practically, a large size can be a limitation in the nodule-to-gland strain. Our study protocol was approved by the Committee of Ethics. All patients gave their informed written consents. Complete history taking was performed including age, sex and symptoms. Full dedicated general and local clinical examination was done. The patients were operated upon within 7 days of the real-time ultrasound elastographic evaluation.

3. Methods

3.1. Real-time ultrasound elastography

Real-time ultrasound elastography was performed preoperatively for all patients by the same radiologist having more than 7 years of experience in thyroid imaging with EUB 7500 (Hitachi Medical Corporation, Tokyo, Japan) ultrasound system using a 6–14 MHz linear transducer (EUB-L65). The patient was positioned on his or her back with the neck slightly extended over a pillow to prevent over stretching of the neck muscles. The probe was placed on the patient's neck with US gel creating a stand-off pad. Transverse and longitudinal gray-scale US images followed by real-time USE for each nodule were obtained. During gray-scale US examination, the following features were evaluated: the greatest diameter of the nodule as well as the cystic component and the rim calcification if present to ensure the absence of the previously mentioned exclusion criteria.

During elastography, the probe was positioned on the neck while applying compression (light pressure) by hand (the so-called a freehand technique) and avoiding the use of high levels of compression because strong pressure may lead to a misdiagnosis. In addition, the patient was asked to avoid swallowing and hold their breathing during the examination to minimize motion of thyroid gland. Then, images were obtained by applying light repetitive compression at the skin above the targeted thyroid nodule and were followed by decompression. The compressive force optimal to achieve good examination quality for ultrasound elastography was monitored using a graded numeric scale which was displayed on the screen. A value of 3 was required throughout the examination to enable a good evaluation through good examination quality. Moreover, we maintained constant level of compression throughout the examination to obtain consistent results.

A region of interest (ROI) was set by the radiologist for elastography acquisition to position the target nodule at the center of the ROI with adjacent normal tissue to be evaluated optimally provided by color homogeneity within the region of interest. As USE is based on acquiring two US images, one image before tissue compression by the probe and the other one after tissue compression by the probe were obtained. Therein, tissue displacement was tracked by assessing the ultrasound beam propagation using a dedicated software [Extended Combined Autocorrelation Method (Extended CAM); Hitachi Medical Corporation]. Images were displayed in a split-screen

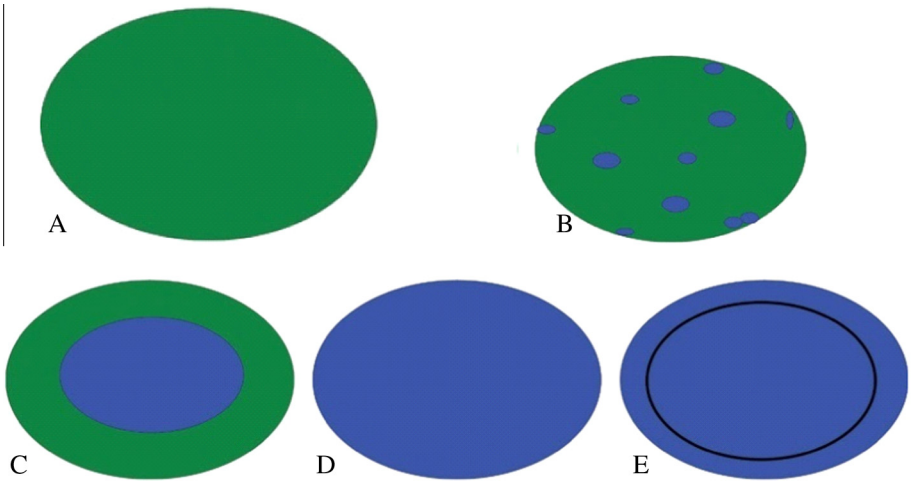

Fig. 1 The applied standard elastography color scoring system according to Rago criteria. (A) A score of 1 indicates even elasticity in the whole nodule. (B) A score of 2 indicates elasticity in a large part of the nodule. (C) A score of 3 indicates elasticity only at the peripheral part of the nodule. (D) A score of 4 indicates no elasticity in the nodule. (E) A score of 5 indicates no elasticity in the nodule or in the area showing posterior shadowing (Quoted from (15)).

mode with the gray-scale images on the right and images of the ultrasound elastogram on the left. The ultrasound elastogram images are produced by superimposing the translucent color-scale images on the corresponding gray-scale US images to easily recognize the relationship between the strain distribution and lesion on B-mode images at a glance.

Each pixel of the elasticity image was shown as one of the 256 specific colors representing the extent of strain. The color scale ranged from red, showing areas of greatest strain or greatest elasticity (i.e., softest component), to blue, showing no strain or no elasticity (i.e., hardest component). The deflections occurring before and after external tissue compression were calculated semiquantitatively and were displayed graphically in the elastogram. Color coding of elastographic images for each nodule was classified according to the score by Rago et al. (13) (hereafter, Rago criteria) on a scale of 1–5 as originated from the elastography scale by Ueno et al. (14) was applied to thyroid nodule. A score of 1 indicates even strain or elasticity in the entire lesion (i.e., the entire lesion is evenly shaded in green as is the surrounding area) (Fig. 1A); a score of 2 indicates strain or elasticity in most of the lesion with some areas of no strain (i.e., a mosaic pattern of green and blue) (Fig. 1B); a score of 3 indicates strain or elasticity only at the peripheral part of the lesion sparing the central part of the lesion (i.e., the peripheral part of the lesion is green and the central part of the lesion is blue) (Fig. 1C); a score of 4 indicates no strain or elasticity in the entire lesion (i.e., the entire lesion is blue but its surrounding area is not included) (Fig. 1D) and a score of 5 indicates no strain or elasticity in the entire lesion or in the surrounding area (i.e., both the entire lesion and its surrounding area are blue) (Fig. 1E) (12,15). The applied standard elastography color scoring system according to Rago criteria is listed in Table 1.

In addition, the strain ratio or strain index (normal tissue to lesion strain ratio) of each nodule was calculated by dividing the strain value (SV) of the normal tissue by that of the nodule (16). The SV was determined by marking the area to be measured on the screen. The SV was calculated from the elastogram as an absolute value. Eventually, the diagnostic performance of USE for differentiation between benign and malignant solitary thyroid nodules using the obtained elastography color scores according to Rago criteria and the measured strain ratio for each nodule was evaluated as regards the final histopathological diagnosis.

Table 1 The applied standard elastography color scoring system according to Rago criteria (Quoted from (12,15)).

Score	Characteristics
1	Even strain or elasticity in the entire lesion (i.e., the entire lesion is evenly shaded in green as is the surrounding area)
2	Strain or elasticity in most of the lesion with some areas of no strain (i.e., a mosaic pattern of green and blue)
3	Strain or elasticity at the peripheral part of the lesion sparing the central part of the lesion (i.e., the peripheral part of the lesion is green and the central part of the lesion is blue)
4	No strain or elasticity in the entire lesion (i.e., the entire lesion is blue but its surrounding area is not included)
5	No strain or elasticity in the entire lesion or in the surrounding area (i.e., both the entire lesion and its surrounding area are blue)

3.2. Histopathological diagnosis

Histopathological examination of all resected thyroid gland tissue specimens was used as the diagnostic standard of reference. It included gross examination of the specimen and microscopic examination of the thyroid nodule as well as the adjacent thyroid parenchyma. Soon after the surgical operation, the tissue specimen was placed in 10% buffered formalin and paraffin embedded for histopathological diagnosis. Four μm thick sections were then prepared and stained with

hematoxylin and eosin. All histopathological diagnoses were made by an expert pathologist who was blinded for the USE parameters. Histopathological diagnoses were defined according to widely recognized guidelines (17).

4. Data analysis

4.1. Statistical analysis

IBM SPSS statistics (V. 21.0, IBM Corp., USA, 2012) was used for data analysis. Data were expressed as mean ± standard deviation (SD) for quantitative parametric measures, in addition to median percentiles for quantitative non-parametric measures and both number and percentage for categorized data. For comparison between two independent mean groups for parametric data, Students's test was used. While, Chi-square test was applied to study the association between each two variables or comparison between two independent

Table 2 The final histopathological diagnosis of the examined thyroid nodules.

Neoplasm type	Number of thyroid nodules
Hyperplastic nodules	15
Follicular adenomas	2
Hashimoto thyroiditis	1
Subacute thyroiditis	3
Papillary carcinomas	9
Medullary carcinomas	2
Follicular carcinomas	3

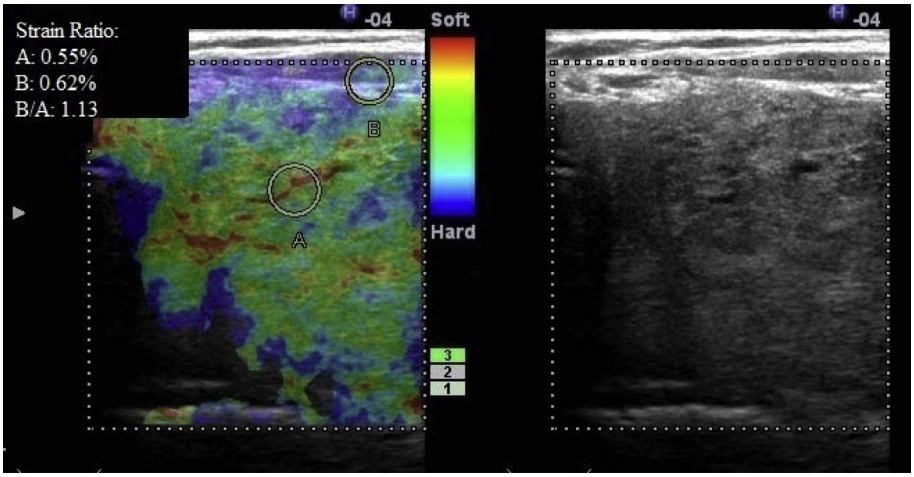

(A)

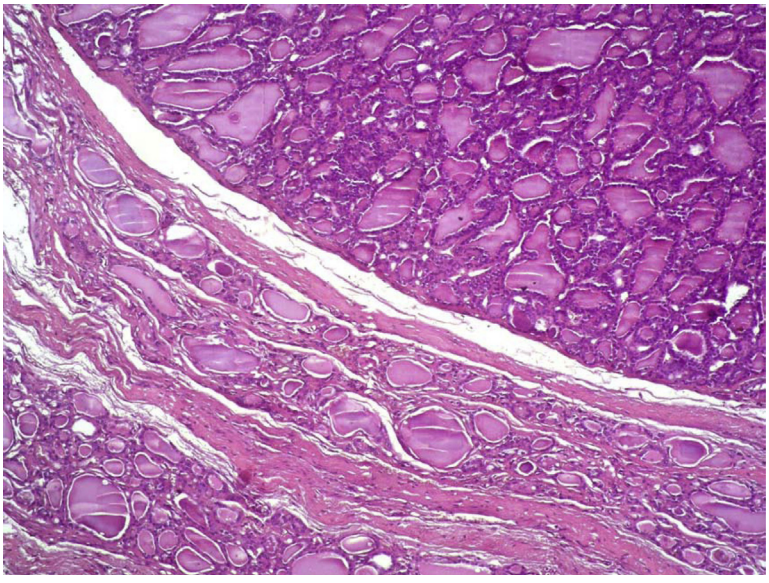

(B)

Fig. 2 (A) Split-screen US elastogram (left) and B-mode ultrasound image (right) show the entire hypoechoic nodule is evenly shaded green as is the surrounding thyroid tissue (a score of 1). The elastogram (left) shows the nodule and normal thyroid tissue of good elasticity (red/yellow) with SV of 0.55% and 0.62% respectively. The strain ratio of the nodule is 1.13 and the grade of compression is 3. (B) Photomicrograph of the histopathological section of the resected thyroid gland tissue reveals a hyperplastic nodule (Hematoxylin-eosin stain; original magnification, ×100).

groups as regards the categorized data. The final histopathological diagnosis was used as the reference standard. The probability of error (p value) at 0.05 was considered significant, while, at 0.01 and 0.001 was considered highly significant. In addition, the diagnostic validity test was used to calculate the sensitivity, specificity, positive predictive value, negative predictive value and diagnostic accuracy or efficacy. Alternatively, receiver operating characteristic (ROC) analysis was constructed to obtain the best cut-off value for the strain ratio.

5. Results

5.1. Demographic and histopathological characteristics

35 thyroid nodules were examined in this prospective study. 25 patients with 1 thyroid nodule for each underwent lobectomy and isthmectomy and 5 patients with 2 nodules for each (one in each lobe) underwent total thyroidectomy. The mean age of patients with malignant nodules was 37.8 ± 5.1 years, while, that of patients with benign nodules was 42.6 ± 7.2 years. Consequently, there was a significant difference ($p < 0.05$) between the mean age of patients with malignant nodules and that of patients with benign nodules. On the other hand, there was no significant difference ($p > 0.05$) regarding sex distribution among patients with benign and malignant solitary thyroid nodules. Patients with malignant nodules comprised 5 males and 9 females. Likewise, patients with benign nodules comprised 4 males and 12 females.

5.2. Histopathological examination

Histopathological examination of the 35 nodules revealed 21 benign nodules (60%) and 14 malignant nodules (40%). The benign nodules comprised 15 hyperplastic nodules, 2 follicular adenomas, 1 Hashimoto thyroiditis nodule and 3 subacute thyroiditis nodules. On the other hand, the malignant nodules comprised 9 papillary carcinomas, 2 medullary carcinomas and 3 follicular carcinomas (Table 2).

5.3. Real-time ultrasound elastography

As color coding of elastographic images was classified into five scores according to Rago criteria; among the 21 benign nodules, 15 nodules (71.4%) had scores of 1 and 2; 5 nodules

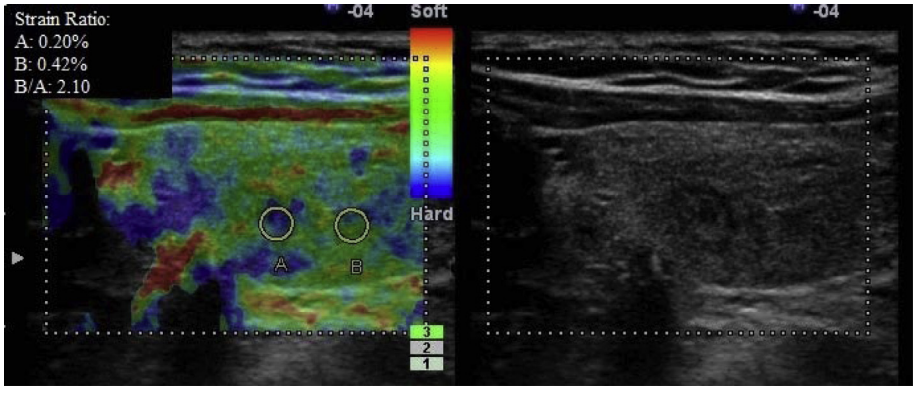

(A)

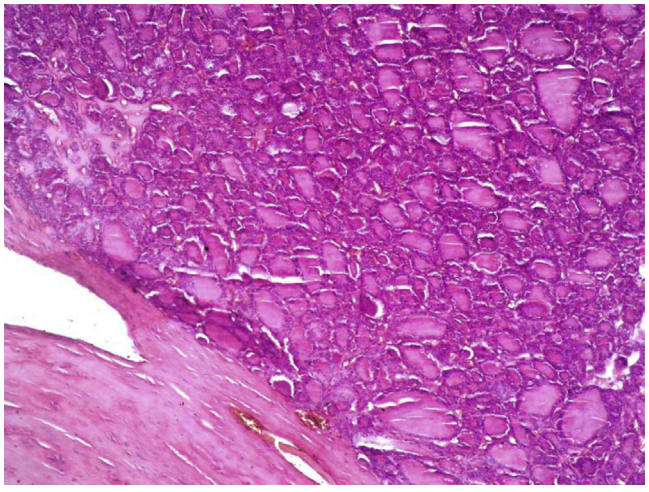

(B)

Fig. 3 (A) Split-screen US elastogram (left) and B-mode ultrasound image (right) show the hypoechoic nodule having mosaic pattern of green and blue (a score of 2). The elastogram (left) shows the nodule and normal thyroid tissue of good elasticity (red/yellow) with SV of 0.20% and 0.42% respectively. The strain ratio of the nodule is 2.10 and the grade of compression is 3. (B) Photomicrograph of the histopathological section of the resected thyroid gland tissue reveals a hyperplastic nodule (Hematoxylin-eosin stain; original magnification, ×100).

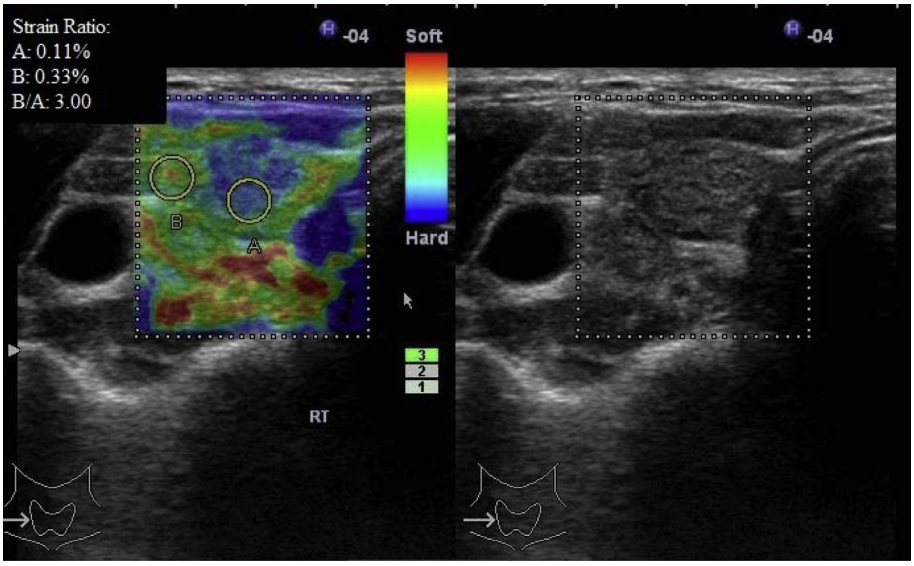

(A)

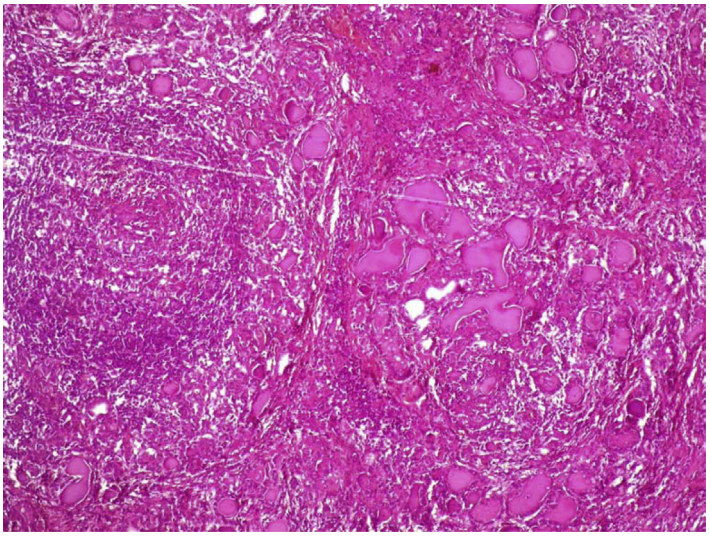

(B)

Fig. 4 (A) Split-screen US elastogram (left) and B-mode ultrasound image (right) show the central part of the hypoechoic nodule in blue and the peripheral part of the nodule in green (a score of 3). The elastogram (left) shows the nodule of low elasticity (blue) apart from its periphery with SV of 0.11% and normal thyroid tissue of good elasticity (red/yellow) with SV of 0.33%. The strain ratio of the nodule is 3.00 and the grade of compression is 3. (B) Photomicrograph of the histopathological section of the resected thyroid gland tissue reveals Hashimoto thyroiditis. It exhibits large lymphoid follicle with prominent germinal center and atrophic thyroid follicles (Hematoxylin-eosin stain; original magnification, ×100).

(23.8%) had a score of 1 (Fig. 2) and 10 nodules (47.6%) had a score of 2 (Fig. 3). Of the 21 benign nodules, 6 nodules (28.6%) had a score of 3 including 3 nodules of subacute thyroiditis, 1 nodule of Hashimoto thyroiditis (Fig. 4) and 2 nodules of follicular adenoma (Fig. 5). None of the benign nodules had a color score of 4 or 5. Among the 14 malignant nodules, 3 nodules of the malignant nodules (21.4%) which comprised follicular carcinoma had a score of 3 (Fig. 6) and 11 nodules (78.6%) had scores of 4 and 5; 3 nodules (21.4%) had a score of 4 (Figs. 7 and 8) and 8 nodules (57.2%) had a score of 5 (Fig. 9). None of the malignant nodules had a color score 1 or 2 (Table 3). Accordingly, scores of 1 and 2 with Rago criteria were highly significant seen in benign nodules, whereas, scores of 4 and 5 with Rago criteria were highly significant seen in malignant nodules ($p < 0.001$). Furthermore, the diagnostic validity test showed that scores 4 and 5 with Rago criteria were predictive of malignancy with a sensitivity of 78.6%; while, scores 1 and 2 with Rago criteria were predictive of benign disease with a specificity of 78.9%. The positive predictive value for malignancy was 73.3%, while, the negative predictive value for benign disease was 83.3% and the diagnostic accuracy or efficacy was 78.8%.

By using ROC analysis for the strain ratio to discriminate between benign and malignant solitary thyroid nodules (Fig. 10), the best strain ratio cut-off value was 2.20. The area under the curve was 0.861, Odd's ratio (95% confidence interval) was 57.0 (7.06–460.4) and p was <0.001. This means in other words that a strain ratio >2.20 identified malignant nodules and a strain ratio $\leqslant 2.20$ identified benign nodules having a consequential sensitivity of 85.7%, specificity of 90.5%, positive predictive value of 85.7%, negative predictive value of 90.5% and diagnostic accuracy or efficacy of 88.6%. Among malignant thyroid nodules ($n = 14$); 2 nodules (14.3%) had a strain ratio $\leqslant 2.20$ and 12 nodules (85.7%) had a strain ratio >2.20. Alternatively, among those benign nodules ($n = 21$); 19 nodules (90.5%) had a strain ratio $\leqslant 2.20$ and 2 nodules (9.5%) had a strain ratio >2.20 (Table 4).

6. Discussion

A number of different diagnostic approaches have been proposed including radionuclide scanning with technetium-99m methylisobutylnitrile (Tc-99m MIBI) and Fluorodeoxyglucose positron-emission tomography (FDG-PET); however, they turned out to be poor predictors of malignancy and of limited clinical efficacy (18,19). In addition, recent guidelines have mentioned that FNAB should not to be performed for all thyroid nodules (5) and US examination represents the main tool in risk stratification of palpable and non palpable lesions and their selection for fine needle aspiration (20,21). Currently, elastography has been introduced to augment the diagnostic accuracy of gray-scale ultrasound (22). Furthermore, it has been established that the thyroid gland is well-positioned for elastographic examination being easily assessed and efficiently

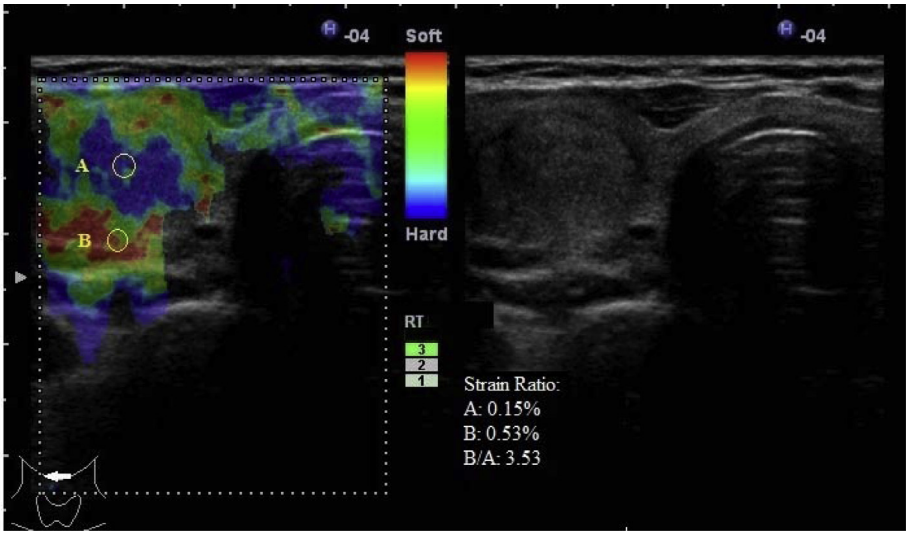

(A)

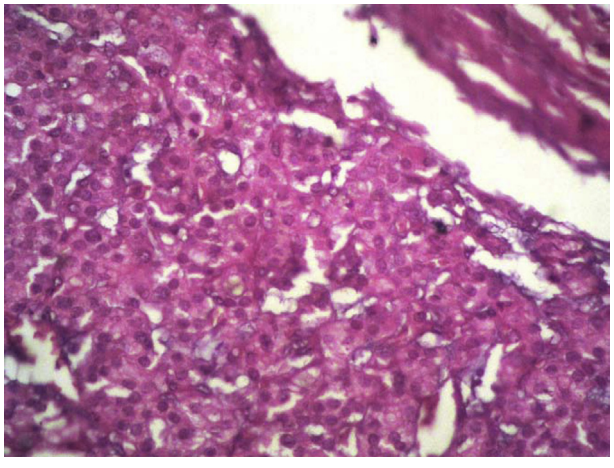

(B)

Fig. 5 (A) Split-screen US elastogram (left) and B-mode ultrasound image (right) show the central part of the hypoechoic nodule in blue and the peripheral part of the nodule in green (a score of 3). The elastogram (left) shows the nodule of low elasticity (blue) apart from its periphery with SV of 0.15% and normal thyroid tissue of good elasticity (red/yellow) with SV of 0.53%. The strain ratio of the nodule is 3.53 and the grade of compression is 3. (B) Photomicrograph of the histopathological section of the resected thyroid gland tissue reveals follicular adenoma of microglandular pattern (Hematoxylin-eosin stain; original magnification, ×400).

compressed against underlying anatomic structures with an ultrasound probe (10).

In this study, we used real-time USE which has proven to be far more advantageous in clinical application (7) as it is simple requiring little time during routine US examinations (23). Real-time USE also gives available immediate results and facilitates the dynamic visualization of lesions during compression with the calculation of the degree of the soft tissue deformation which is combined with a gray-scale US image as an elastography map (8). As well, we performed real-time USE using external compression like most studies in which the elastographic image is created by a slight raising and lowering movement with the transducer and the elastogram is generated in real-time. In other studies, the pulsation of carotid artery was used as the compression source (24,25) or the elastogram was generated off-line (26). Both are associated with high costs in terms of time and technology (7).

Regarding carotid artery pulsation approach, it has been claimed that this approach would be advantageous over external compression by having inherent periodic pulsation (i.e., expansion and contraction of the carotid artery lumen diameter during systole and diastole) and its position (adjacent to the thyroid). In addition, intrinsic compression could eliminate the variability caused by different compression levels applied by the operators with external compression elastography (24,25). However, it has also been reported that arterial pulsations may generate compression–decompression movements which in turn may create unnecessary thyroid movement interfering with elastographic images and is difficult to be

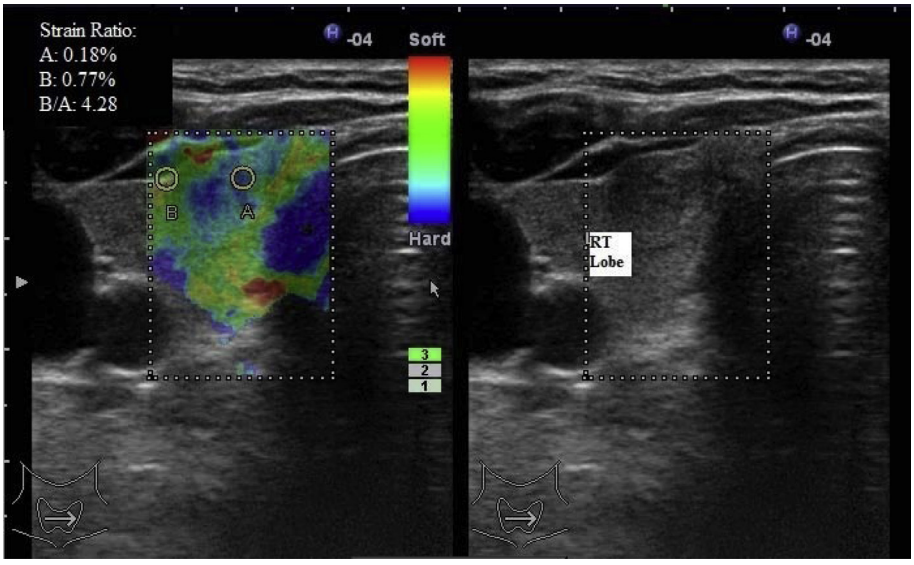

(A)

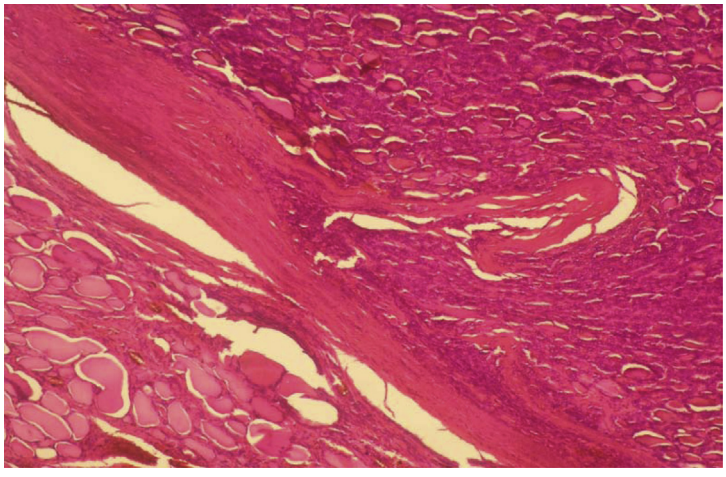

(B)

Fig. 6 (A) Split-screen US elastogram (left) and B-mode ultrasound image (right) show the central part of the hypoechoic nodule in blue and the peripheral part of the nodule in green (a score of 3). The elastogram (left) shows the nodule of low elasticity (blue) apart from its periphery with SV of 0.18% and normal thyroid tissue of good elasticity (red/yellow) with SV of 0.77%.The strain ratio of the nodule is 4.28 and the grade of compression is 3. (B) Photomicrograph of the histopathological section of the resected thyroid gland tissue reveals the capsular invasion of follicular carcinoma (Hematoxylin-eosin stain; original magnification, ×100).

restricted (23). Therefore, in our study, we did not use carotid artery pulsation as a compression source.

We applied compression (light pressure) and avoided using high levels of compression as it is well known that the association between compression and strain in high levels of compression is no longer proportional (23). Thus, the freehand compression applied on the neck region in our study was standardized by real-time measurement to be maintained throughout the examination constant at an intermediate level optimal for US elastographic evaluation. In addition, this has the benefit of minimizing the variability whether interobserver (to prevent differences among operators) and intraobserver (to standardize the degree of nodule compression) and hence, the benefit of obtaining reliable results (13).

To our knowledge, although several studies have evaluated this technique, surgical intervention was performed only in a limited number of studies (10,13,23,25,26). As a result, deficiency of surgical confirmation in the majority hampers to some extent a wider range of conclusions. Conversely, we adequately defined the selection; in addition, the final histopathological diagnosis was supplemented to all included patients. Furthermore, recent advances in elastography allow quantification using the strain ratio calculated as the ratio of stiffness between nodular tissue versus surrounding normal thyroid tissue (27). Consequently, we utilized this latest generation of real-time USE to differentiate between benign and malignant solitary thyroid nodules using the color scale and by measuring the stain ratio using SV, the absolute value, which quantifies

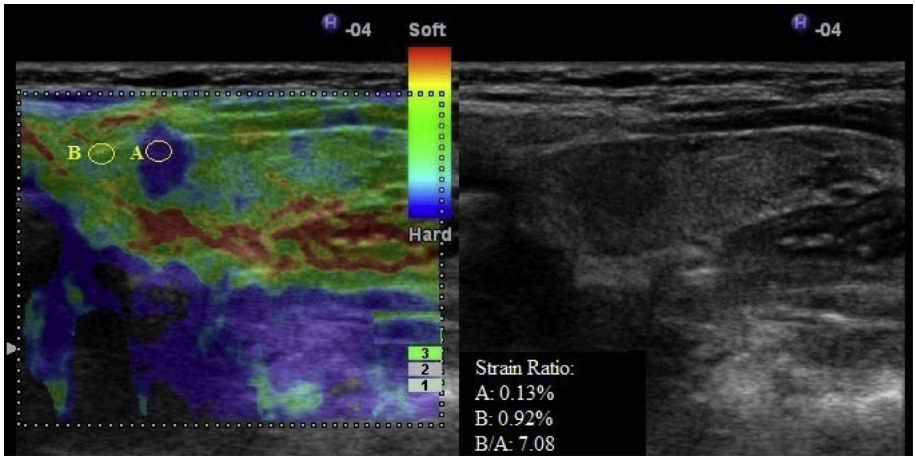

(A)

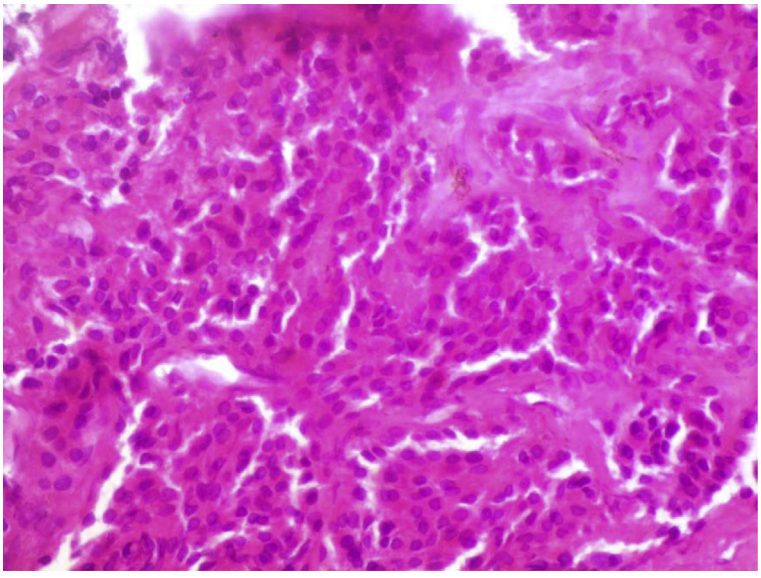

(B)

Fig. 7 (A) Split-screen US elastogram (left) and B-mode ultrasound image (right) show the entire hypoechoic nodule in blue (a score of 4). The elastogram (left) shows the nodule of low elasticity (blue) with SV of 0.13% and normal thyroid tissue of good elasticity (red/yellow) with SV of 0.92%. The strain ratio of the nodule is 7.08 and the grade of compression is 3. (B) Photomicrograph of the histopathological section of the resected thyroid gland tissue reveals medullary carcinoma with amyloid deposition (Hematoxylin-eosin stain; original magnification, ×400).

nodule stiffness as an advantage of clear reproducibility and assignment (7).

We purposely evaluated the diagnostic performance of the latest generation of real-time USE as an individual variable. Herein, the use of gray-scale US maintained a substantial importance to ensure the absence of exclusion criteria which represent the technical limits of real-time USE technique as follows. The main determinant of nodule stiffness is the fluid content and not the solid wall (13). Additionally, the classic elastogram for a cyst consists of three color layers (blue–green–red) from top to bottom (28). On the other hand, macrocalcifications (either coarse or shell calcifications) have a hard blue appearance at real-time USE (29), as the US beam does not cross the calcification (13) and the compression does not result in tissue strain deformation (30).

The final diagnosis which was proved by histopathology showed that 40% of the included thyroid nodules had malignancy. This is in agreement with the obtained result of 21–54% in previous studies (10,13,26,30). The high prevalence of malignant nodules in the present study is due to the enrollment of patients referred by primary oncology centers for undergoing surgery and to the exclusion criteria of purely cystic and the peripherally calcified nodules. Even a higher prevalence of malignancy of 62.2% was found in the study done by Mohamed and Abodewan (31).

We used the elastography color scoring system according to Rago criteria ranging from 1 to 5. Scores of 4 and 5 in our study were highly significant seen in malignant nodules (11 out of 14 nodules) (78.6%). This was consistent with other studies (11,13,15,24,26,30). On the other hand, Hong et al. (10) adopted a scoring system for tissue stiffness on USE ranging from 1 (low stiffness over the entire nodule) to 6 (high stiffness over the entire nodule and surrounding tissue). They found that 86 of 96 benign nodules (90%) had a score of 1–3, whereas, 43 of 49 malignant nodules

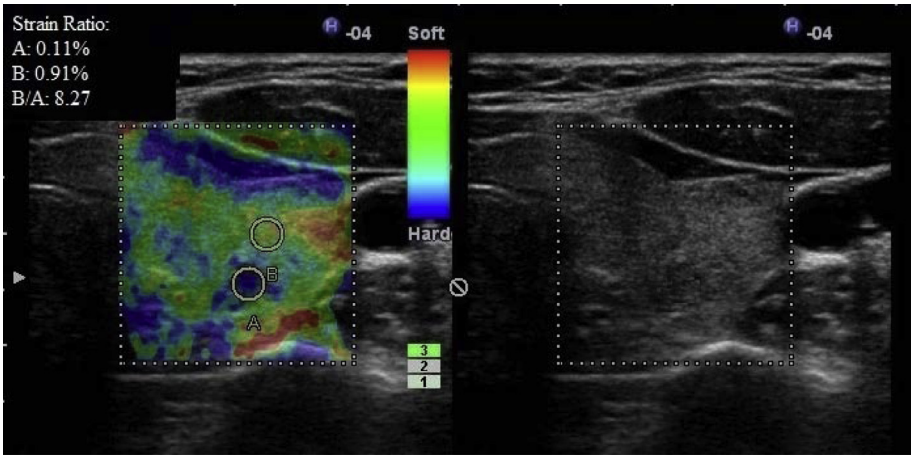

(A)

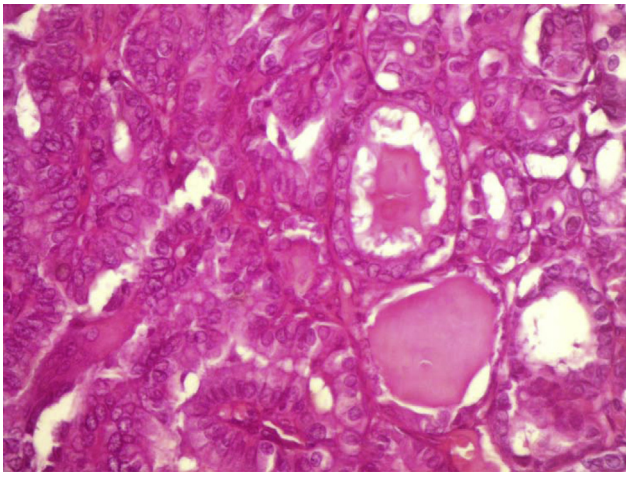

(B)

Fig. 8 (A) Split-screen US elastogram (left) and B-mode ultrasound image (right) show the entire hypoechoic nodule in blue (a score of 4). The elastogram (left) shows the nodule of low elasticity (blue) with SV of 0.11% and normal thyroid tissue of good elasticity (red/yellow) with SV of 0.91%. The strain ratio of the nodule is 8.27 and the grade of compression is 3. (B) Photomicrograph of the histopathological section of the resected thyroid gland tissue reveals follicular variant of papillary carcinoma with its characteristic nuclear features (Hematoxylin-eosin stain; original magnification, ×400).

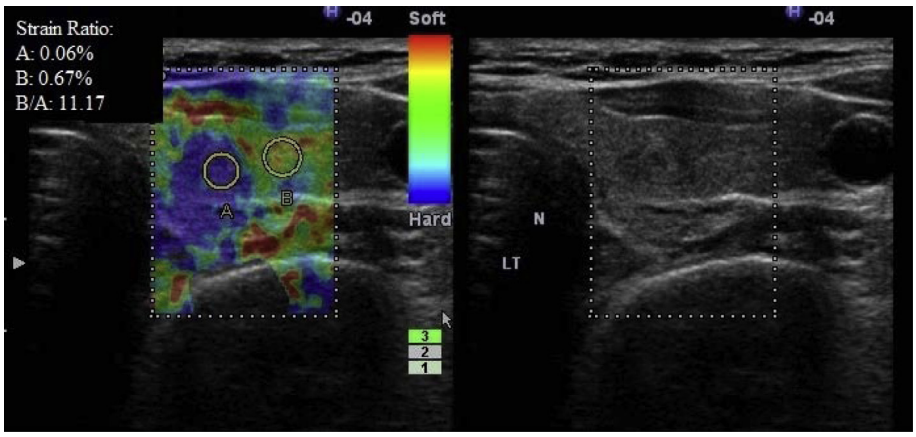

(A)

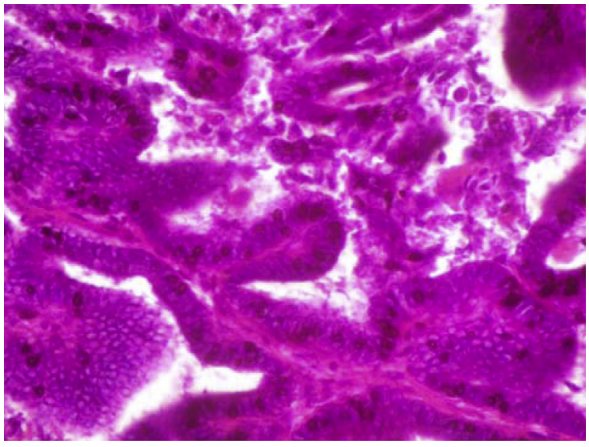

(B)

Fig. 9 (A) Split-screen US elastogram (left) and B-mode ultrasound image (right) show both the entire hypoechoic lesion and its surrounding area in blue (a score of 5). The elastogram (left) shows the nodule of low elasticity (blue) with SV of 0.06% and normal thyroid tissue of good elasticity (red/yellow) with SV of 0.67%. The strain ratio of the nodule is 11.17 and the grade of compression is 3. (B) Photomicrograph of the histopathological section of the resected thyroid gland tissue reveals papillary carcinoma (Hematoxylin-eosin stain; original magnification, ×400).

Table 3 The examined thyroid nodules with the obtained elastography color scores according to Rago criteria.

	Malignant nodules, *n* (%)	Benign nodules, *n* (%)
Scores 1 and 2	0 (0.0)	15 (71.4)
Score 3	3 (21.4)	6 (28.6)
Scores 4 and 5	11 (78.6)	0 (0.0)
Total	14 (100.0)	21 (100.0)

(88%) had a score of 4–6. Likewise, in the study done by Mohamed and Abodewan (31) scores 4–6 were found in 25 of 28 patients (89.3%) having a final diagnosis of malignancy. Whereas, scores of 1–3 were found in 15 out of 17 patients (88.2%) with an ultimate histopathological diagnosis of a benign lesion.

In this study, 9 papillary thyroid carcinomas (100%) had scores of 4 and 5. Similarly, in the study done by Hong et al. (10), 41 of 44 papillary thyroid carcinomas (93%) had a score of 4–6. It is clarified that papillary thyroid carcinoma has complex papillae with a central fibrovascular stalk, in addition to psammoma bodies and fibrosis which are often found in them (32,33). On the other hand, the study performed by Mohamed and Abodewan (31) revealed 1 papillary carcinoma having an elastography score of 3.

It has been reported that USE has an important limitation of probably lacking sensitivity for follicular thyroid carcinoma (30) with the inability to sufficiently differentiate between thyroid follicular carcinoma and follicular adenoma (7). As well, we detected 3 follicular thyroid carcinomas having a score of 3. This result corresponds to the result of the study done by Hong et al. (10) and Mohamed and Abodewan (31). Likewise, Bojunga et al. (11) overlooked 16 of the 153 final thyroid malignancies including four of the nine follicular carcinomas (44%). The gross anatomy and cellular patterns of follicular carcinoma overlap with those of benign follicular adenoma. Nevertheless, this kind of thyroid malignancy can be differentiated from benign follicular adenoma only when capsular or vascular invasion are discovered at histologic examination (34–36).

USE in this study showed a sensitivity of 78.6% and a specificity of 78.9%. The sensitivity and specificity of USE

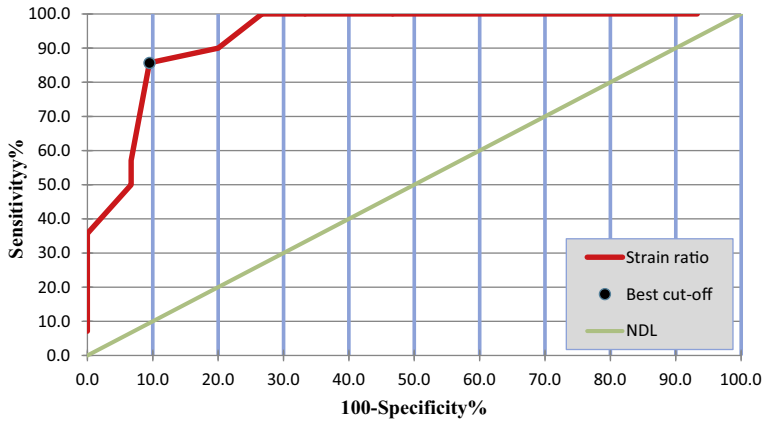

Fig. 10 Receiver operating characteristic (ROC) analysis for the strain ratio to discriminate between benign and malignant solitary thyroid nodules. The best strain ratio cut-off value was 2.20 and the area under the curve was 0.861. NDL (non diagnostic line).

Table 4 The number and percentage of the examined thyroid nodules using the best strain ratio cut-off value of 2.20 for discrimination between benign and malignant solitary thyroid nodules.

	Malignant nodules, *n* (%)	Benign nodules, *n* (%)
Strain ratio >2.20	12 (85.7)	2 (9.5)
Strain ratio ⩽2.20	2 (14.3)	19 (90.5)
Total	14 (100.0)	21 (100.0)

for differentiating thyroid nodules have been reported to be 82–97% and 77.5–100% respectively (10,11,13,24,26,30). Mohamed and Abodewan (31) had a diagnostic accuracy of 88.9%. This is compared to our result of a diagnostic accuracy of 78.8%.

Our results regarding the strain ratio confirmed previous studies (11,24,37) by demonstrating that malignant nodules have a significantly higher stiffness compared to benign ones. In addition, we found that the best strain ratio cut-off value for discriminating between benign and malignant nodules was 2.20 with 85.7% sensitivity, 90.5% specificity and 88.6% diagnostic accuracy. Correspondingly, the sensitivity, specificity and diagnostic accuracy of the strain index values were 85.7%, 82.1% and 82.4%, respectively, when the best cut-off point of 2.31 was used (8). As well, Cantisani et al. (37) obtained a best strain ratio cut-off value of 2.05 for discriminating between benign and malignant lesions with 87.5% sensitivity, 92% specificity and 89.8% diagnostic accuracy. On the other hand, Kagoya et al. (6) found that a strain ratio greater than 1.5 was set as the predictor of thyroid malignancy with 90% sensitivity and 50% specificity. Other researchers suggested a strain index value greater than 4 as the strongest independent factor in predicting malignancy of nodules with 82% sensitivity and 96% specificity (26).

Alternatively, some benign nodules may have increased stiffness. In our study, 1 nodule with the histopathological diagnosis of Hashimoto thyroiditis and 3 nodules with the histopathological diagnosis of subacute thyroiditis had a score of 3. Most of the follicular epithelium in subacute thyroiditis is replaced by a rim of histiocytes and giant cells, interstitial fibrosis and infiltration of lymphocytes and plasma cells (34). Moreover, Hong et al. (10) reported that two nodules in patients with subacute thyroiditis showed malignant USE finding. Yet, Dighe et al. (24) reported benign USE results in four patients with lymphocytic thyroiditis.

Finally, we recommend further studies with a larger population to confirm our USE findings in differentiation between benign and malignant solitary thyroid nodules of various pathological entities and to ascertain the diagnostic accuracy of this technique. As this aims for better patient's triage by reducing the number of superfluous surgical procedures on benign thyroid nodules and by allowing prompt management and hence, improving the prognosis through detecting malignancy at an early stage.

To conclude, real-time ultrasound elastography should not be applied to any thyroid nodules but should be restricted to thyroid nodules having no technical limits for this modality. This is ensured by gray-scale ultrasound to define which nodules are suitable for the ultrasound elastographic characterization. The use of color score and strain ratio reveals that high elasticity is markedly associated with benign histopathology and low elasticity is markedly associated with malignant histopathology. Accordingly, real-time ultrasound elastography seems to have a great diagnostic potential for differentiating benign and malignant solitary thyroid nodules. This in turn reduces the number of unnecessary surgical procedures on benign thyroid nodules.

Conflict of interest

The authors have no conflict of interest to declare.

References

(1) Knox MA. Thyroid nodules. Am Fam Physician 2013;88(3):193–6.
(2) Lim D-J, Luo S, Kim M-H, et al. Interobserver agreement and intraobserver reproducibility in thyroid ultrasound elastography. AJR 2012;198(4):896–901.
(3) Hegedüs L. Clinical practice. The thyroid nodule. N Engl J Med 2004;351(17):1764–71.

(4) Hegedüs L, Bonnema SJ, Bennedbaek FN. Management of simple nodular goiter: current status and future perspectives. Endocr Rev 2003;24(1):102–32.
(5) Gharib H, Papini E, Paschke R, et al. AACE/AME/ETA task force on thyroid nodules. American Association of Clinical Endocrinologists, Associazione Medici Endocrinologi, and European Thyroid Association medical guidelines for clinical practice for the diagnosis and management of thyroid nodules. Endocr Pract 2010;16(Suppl. 1):1–43.
(6) Kagoya R, Monobe H, Tojima H. Utility of elastography for differential diagnosis of benign and malignant thyroid nodules. Otolaryngol Head Neck Surg 2010;143(2):230–4.
(7) Vorländer C, Wolff J, Saalabian S, et al. Real-time ultrasound elastography—a noninvasive diagnostic procedure for evaluating dominant thyroid nodules. Langenbecks Arch Surg 2010; 395(7):865–71.
(8) Çiledag N, Arda K, Aribas BK, et al. The utility of ultrasound elastography and MicroPure imaging in the differentiation of benign and malignant thyroid nodules. AJR 2012;198(3): W244–9.
(9) Hegedüs L. Can elastography stretch our understanding of thyroid histomorphology? J Clin Endocrinol Metab 2010;95(12): 5213–5.
(10) Hong Y, Liu X, Li Z, et al. Real-time ultrasound elastography in the differential diagnosis of benign and malignant thyroid nodules. J Ultrasound Med 2009;28(7):861–7.
(11) Bojunga J, Herrmann E, Meyer G, et al. Real-time elastography for the differentiation of benign and malignant thyroid nodules: a meta-analysis. Thyroid 2010;20(10):1145–50.
(12) Itoh A, Ueno E, Tohno E, et al. Breast disease: clinical application of US elastography for diagnosis. Radiology 2006; 239(2):341–50.
(13) Rago T, Santini F, Scutari M, et al. Elastography: new developments in ultrasound for predicting malignancy in thyroid nodules. J Clin Endocrinol Metab 2007;92(8):2917–22.
(14) Ueno E, Itoh A. Diagnosis of breast cancer by elasticity imaging. Eizo Joho Med 2004;36(12):2–6.
(15) Moon HJ, Sung JM, Kim E-K, et al. Diagnostic performance of gray-scale US and elastography in solid thyroid nodules. Radiology 2012;262(3):1002–13.
(16) Cantisani V, D'Andrea V, Biancari F, et al. Prospective evaluation of multiparametric ultrasound and quantitative elastosonography in the differential diagnosis of benign and malignant thyroid nodules: preliminary experience. Eur J Radiol 2012;81(10):2678–83.
(17) Nikiforov YE, Biddinger PW, Thompson LDR. Diagnostic pathology and molecular genetics of the thyroid. A comprehensive guide for practicing thyroid pathology. 2nd ed. Philadelphia, PA: Wolters Kluwer Health, Lippincott Williams & Wilkins; 2012.
(18) Leidig-Bruckner G, Cichorowski G, Sattler P, et al. Evaluation of thyroid nodules – combined use of 99mTc-methylisobutylnitrile scintigraphy and aspiration cytology to assess risk of malignancy and stratify patients for surgical or nonsurgical therapy – a retrospective cohort study. Clin Endocrinol (Oxf) 2012;76(5):749–58.
(19) Deandreis D, Al Ghuzlan A, Auperin A, et al. Is 18F-fluorodeoxyglucose–PET/CT useful for the presurgical characterization of thyroid nodules with indeterminate fine needle aspiration cytology? Thyroid 2012;22(2):165–72.
(20) Gharib H, Papini E, Paschke R, et al. AACE/AME/ETA Task Force on thyroid nodules. American Association of Clinical Endocrinologists, Associazione Medici Endocrinologi, and European Thyroid Association medical guidelines for clinical practice for the diagnosis and management of thyroid nodules. J Endocrinol Invest 2010;33(5 Suppl.):1–50.
(21) Cooper DS, Doherty GM, Haugen BR, et al. American Thyroid Association Guidelines Taskforce. Management guidelines for patients with thyroid nodules and differentiated thyroid cancer. Thyroid 2006;16(2):109–42.
(22) Gao L, Parker KJ, Lerner RM, et al. Imaging of the elastic properties of tissue–a review. Ultrasound Med Biol 1996;22(8): 959–77.
(23) Park SH, Kim SJ, Kim E-K, et al. Interobserver agreement in assessing the sonographic and elastographic features of malignant thyroid nodules. AJR 2009;193(5):W416–23.
(24) Dighe M, Bae U, Richardson ML, et al. Differential diagnosis of thyroid nodules with US elastography using carotid artery pulsation. Radiology 2008;248(2):662–9.
(25) Bae U, Dighe M, Dubinsky T, et al. Ultrasound thyroid elastography using carotid artery pulsation: preliminary study. J Ultrasound Med 2007;26(6):797–805.
(26) Lyshchik A, Higashi T, Asato R, et al. Thyroid gland tumor diagnosis at US elastography. Radiology 2005;237(1):202–11.
(27) Ning C-P, Jiang S-Q, Zhang T, et al. The value of strain ratio in differential diagnosis of thyroid solid nodules. Eur J Radiol 2012;81(2):286–91.
(28) Carlsen JF, Ewertsen C, Lönn L, et al. Strain elastography ultrasound: an overview with emphasis on breast cancer diagnosis. Diagnostics 2013;3(1):117–25.
(29) Trimboli P, Guglielmi R, Monti S, et al. Ultrasound sensitivity for thyroid malignancy is increased by real-time elastography: a prospective multicenter study. J Clin Endocrinol Metab 2012; 97(12):4524–30.
(30) Asteria C, Giovanardi A, Pizzocaro A, et al. US-elastography in the differential diagnosis of benign and malignant thyroid nodules. Thyroid 2008;18(5):523–31.
(31) Mohamed RE, Abodewan KA. Diagnostic utility of real-time ultrasound elastography for prediction of malignancy in solid thyroid nodules. Egypt J Radiol Nucl Med 2013;44(1):33–43.
(32) Reading CC, Charboneau JW, Hay ID, et al. Sonography of thyroid nodules: a "classic pattern" diagnostic approach. Ultrasound Q 2005;21(3):157–65.
(33) Carcangiu ML, Zampi G, Rosai J. Papillary thyroid carcinoma: a study of its many morphologic expressions and clinical correlates. Pathol Annu 1985;20(Pt 1):1–44.
(34) McNicol AM. Pathology of thyroid tumours. Surgery (Oxf) 2007;25(11):458–62.
(35) Rago T, Di Coscio G, Basolo F, et al. Combined clinical, thyroid ultrasound and cytological features help to predict thyroid malignancy in follicular and Hürthle cell thyroid lesions: results from a series of 505 consecutive patients. Clin Endocrinol (Oxf) 2007;66(1):13–20.
(36) Maizlin ZV, Wiseman SM, Vora P, et al. Hürthle cell neoplasms of the thyroid: sonographic appearance and histologic characteristics. J Ultrasound Med 2008;27(5):751–7.
(37) Cantisani V, Ulisse S, Guaitoli E, et al. Q-elastography in the presurgical diagnosis of thyroid nodules with indeterminate cytology. PLoS One 2012;7(11):e50725.